

Electronic Supporting Information

***In situ* XAS study of the local structure and oxidation state evolutions of palladium in a reduced graphene oxide supported Pd(II) carbene complex during an undirected C–H acetoxylation reaction**

Ning Yuan, *†^{a,b} Maitham H. Majeed, †^c Éva G. Bajnóczi, ^a Axel R. Persson, ^{c,d} L. Reine Wallenberg, ^{c,d} A. Ken Inge, ^b Niclas Heidenreich, ^{e,f} Norbert Stock, ^e Xiaodong Zou, ^b Ola F. Wendt, ^{*c} and Ingmar Persson ^{*a}

- Department of Molecular Sciences, Swedish University of Agricultural Sciences, P.O. Box 7015, SE-750 07 Uppsala, Sweden
- Department of Materials and Environmental Chemistry, Stockholm University, SE-106 91 Stockholm, Sweden
- Centre for Analysis and Synthesis, Department of Chemistry, Lund University, P.O. Box 124, SE-221 00 Lund, Sweden
- National Centre for High Resolution Electron Microscopy and NanoLund, Lund University, P. O. Box 124, SE-221 00 Lund, Sweden
- Institut für Anorganische Chemie, Christian-Albrechts-Universität zu Kiel, DE-24118 Kiel, Germany
- Deutsches-Elektronen-Synchrotron DESY, DE-22607 Hamburg, Germany

† These authors contributed equally to this work.

Contents

| | |
|--|----|
| Section S1. XAS data collection and analysis | 2 |
| Section S2. Additional XANES spectra | 3 |
| Section S3. EXAFS spectra refinement of as-synthesized 1 @rGO and 1 , and the catalysts during <i>in situ</i> measurements. | 4 |
| Section S4. Transmission electron microscopy images of recycled 1 @rGO..... | 9 |
| References | 11 |

Section S1. XAS data collection and analysis

X-ray absorption spectroscopy (XAS) data were collected at the undulator based beamline P64 which is equipped with a Si[311] double crystal monochromator (https://photon-science.desy.de/facilities/petra_iii/beamlines/p64_advanced_xafs/index_eng.html) at Petra III Extension, Deutsches Elektronen-Synchrotron (DESY), Hamburg, Germany. The facility is operating at 6.0 GeV and 100 mA. 60% of the maximum intensity at the end of the scans was reflected to reduce higher order harmonics by detuning the second monochromator crystal. XAS measurements were performed at palladium (Pd) K-edge (24.35 keV) with an energy range from 24.00 to 25.15 keV for dry samples or 25.00 keV for *in situ* measurement in a continuous scanning mode.¹ All XAS data collection was in transmission mode and a Pd foil reference was always measured simultaneously for internal energy calibration with the first inflection point of the absorption edge defined as 24350 eV.¹ Ion chambers were used to monitor the intensities of the incident beam (I_0), sample transmitted beam (I_1) and Pd metal foil transmitted beam (I_2).

The as-synthesized dry **1** and **1**@rGO, as well as the **1**@rGO recycled from the reaction mixture after *in situ* measurement were pelleted for XAS measurements. Each XAS scan was set for ca. 5 min and multiple scans (4-9 scans) were acquired for each sample in consideration of the low loading of Pd in the catalysts (ca. 2.5 wt%). The data was then averaged to improve the S/N ratio before the data analysis.

For the *in situ* XAS measurement the catalysts were mixed with all the reaction components described in Section S2 in a custom made *in situ* reactor (Figure S1).² The test tube in the reactor was positioned perpendicularly to the X-ray beam for maximum distance through the sample and avoid unnecessary scattering. A homogeneous solution or suspension was maintained by magnetic stirring. Each XAS scan was also set at ca. 6 min. with considerations of both time resolution and data quality.

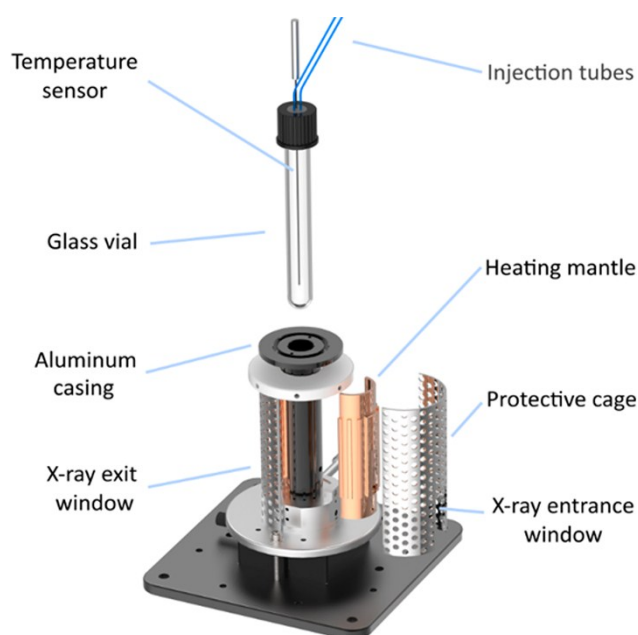


Figure S1. Custom-made reactor for *in situ* XAS. (Reprinted with permission from *J. Am. Chem. Soc.* 2018, 140, 8206-8217. Copyright (2018) American Chemical Society)

The XAS data was divided into two parts, X-ray absorption near edge structure (XANES) and extended X-ray absorption fine structure (EXAFS) regions. The edge position in each XANES spectrum was determined by comparison to the internal calibration with a metallic palladium foil. All XANES spectra were normalized in the same way by fixing the absorbance value of the position exactly between minimum and maximum in the EXAFS wave in Figures 1 and 3 to 1.0. The white line intensity and shape of XANES spectra were then compared. The data treatment of EXAFS spectra was performed with the EXAFSPAK package including pre-edge subtraction, spline removal, normalization and Fourier transformation.³ The experimental k^3 -weighted EXAFS oscillations were analyzed by non-linear least-squares fits of the data to the EXAFS equation, refining the model parameters, number of backscattering atoms (N), mean interatomic distances (R), Debye-Waller factor coefficients (σ^2) and threshold energy (E_0). The *ab initio* program package FEFF7 was used to calculate the theoretical phases and amplitudes.⁴ It should be noticed that the distances read in Fourier transformed EXAFS spectra are without phase correction and true distance values are determined from EXAFS refinements. The standard deviations reported for the refined parameters were obtained from k^3 -weighted least-squares refinements of the EXAFS function $\chi(k)$, and without including systematic errors. For a well-defined interaction, the accuracy of the distances given for an individual complex is between ± 0.005 and ± 0.02 Å.

Section S2. Additional XANES spectra

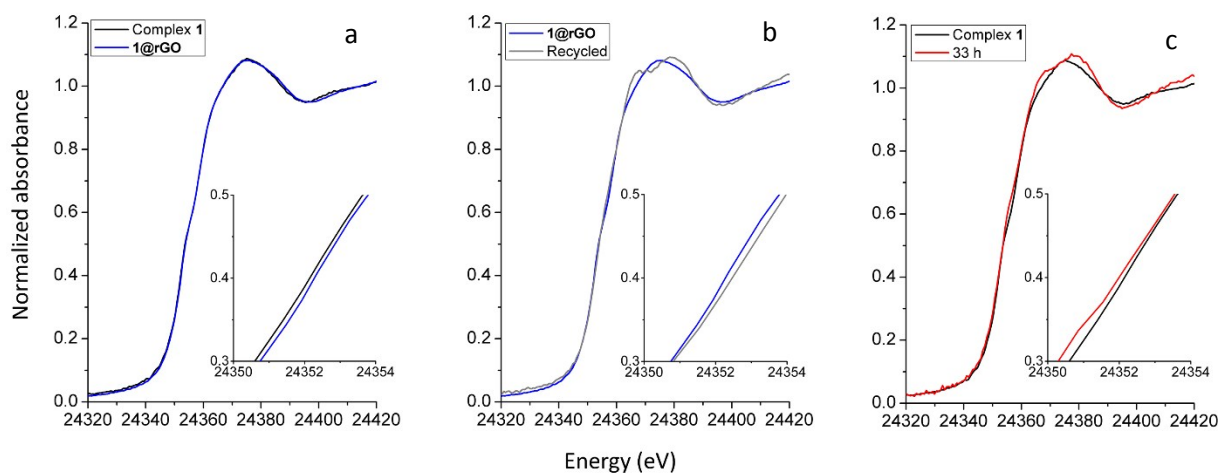


Figure S2. Pd K-edge XANES spectra of (a) as-synthesized **1** and **1@rGO**, (b) as-synthesized **1@rGO** and the recycled **1@rGO**, and (c) as-synthesized **1** and **1** at 33 h of the *in situ* measurement.

Section S3. EXAFS spectra refinement of as-synthesized **1**@rGO and **1**, and the catalysts during *in situ* measurements.

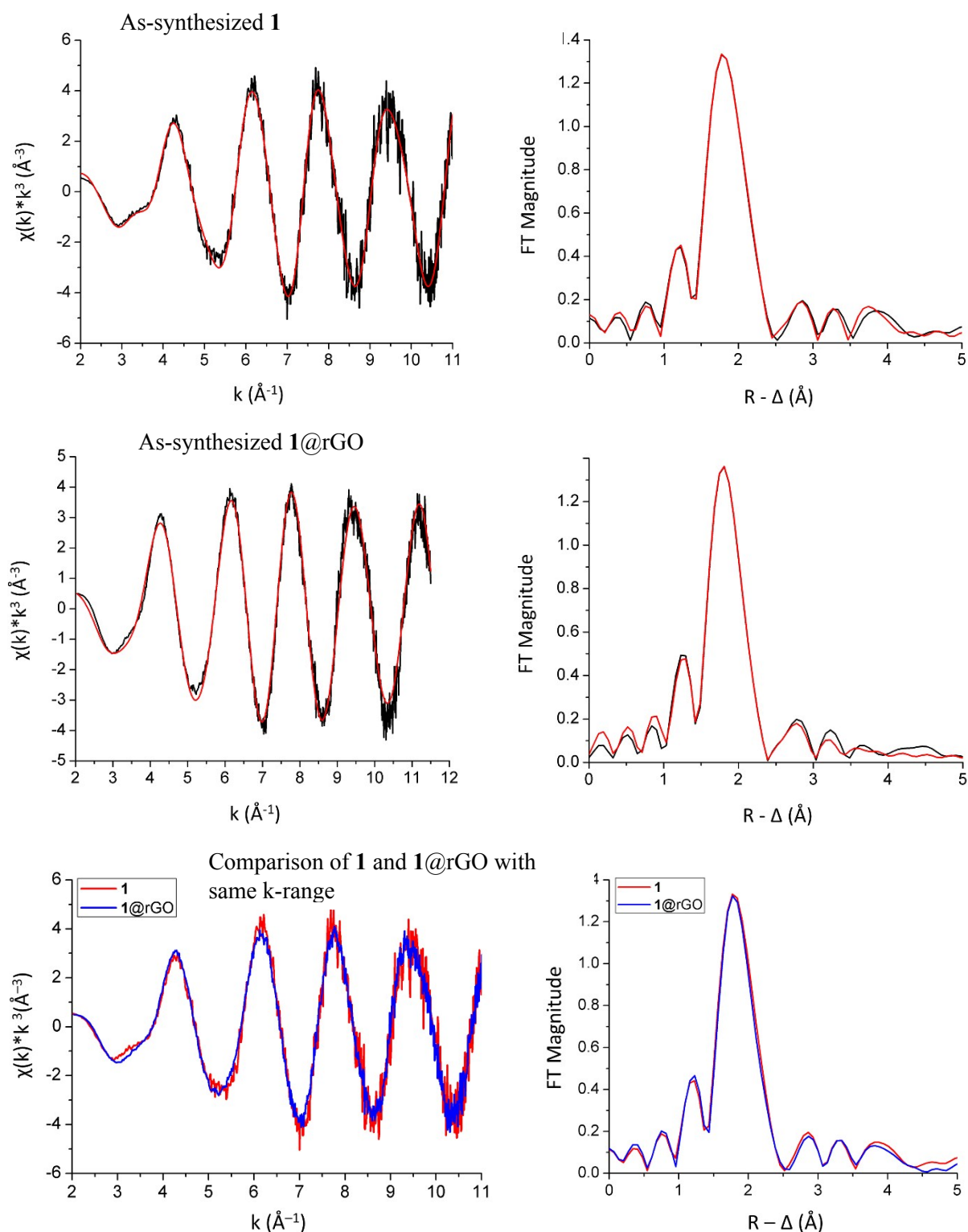
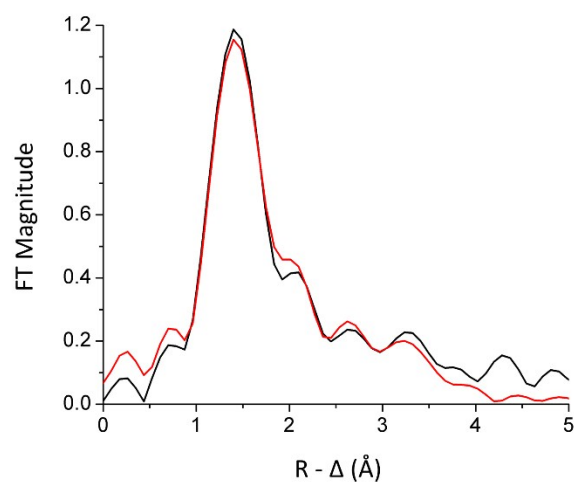
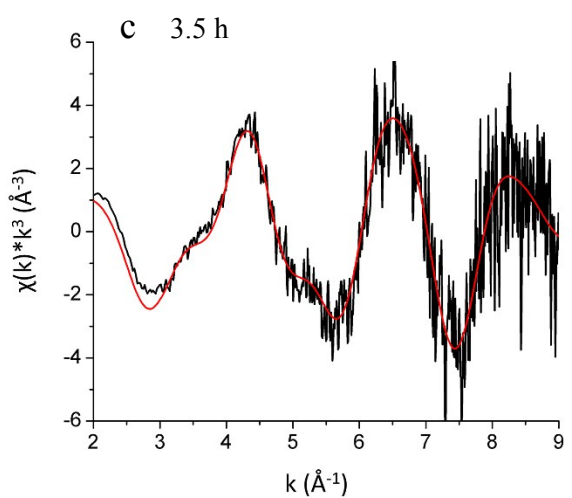
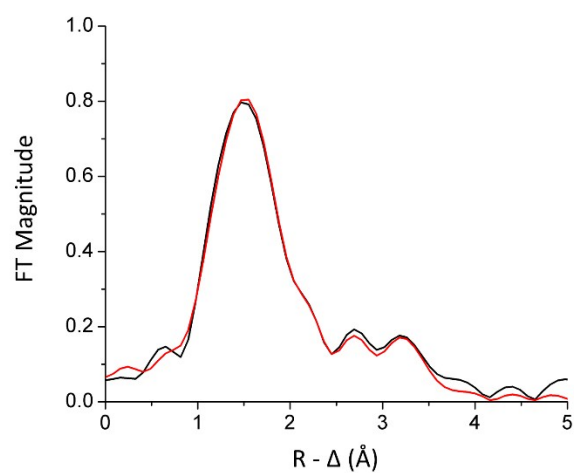
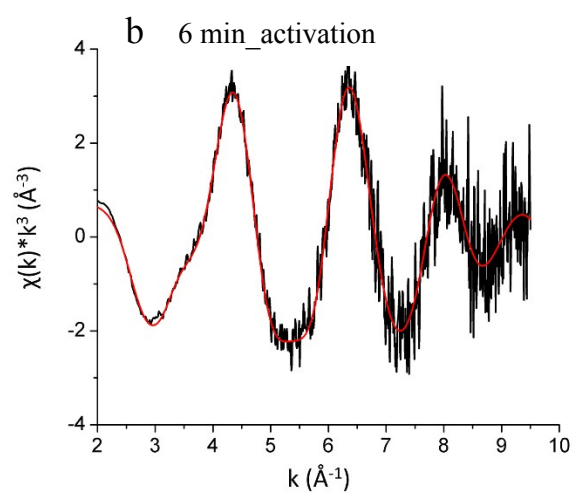
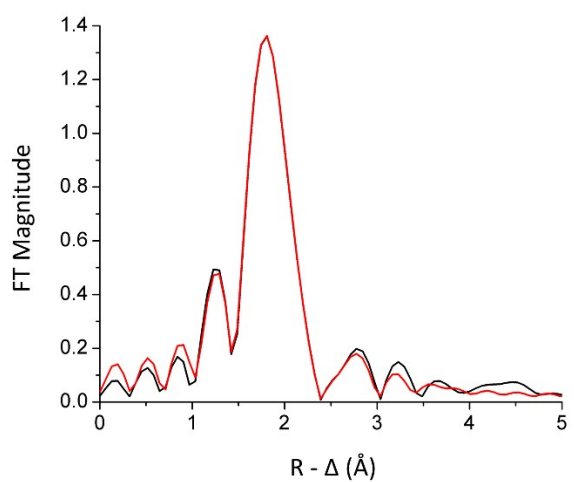
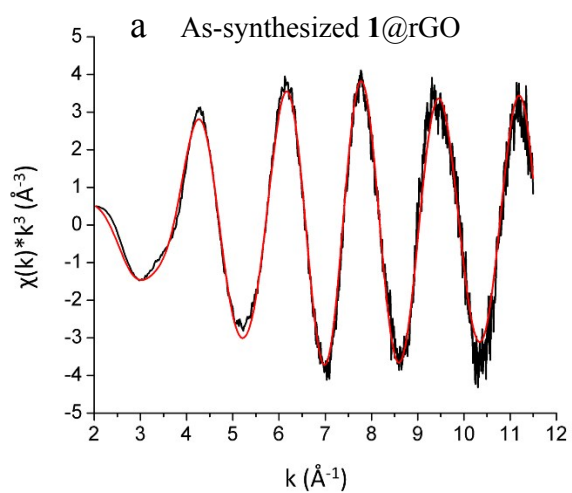


Figure S3. Fit of Pd *K*-edge EXAFS data and its respective Fourier transform for as-synthesized dry **1** (top) and **1**@rGO (bottom), black curve – experimental, red curve – model. The experimental data of **1** and **1**@rGO with same *k*-range (2 – 11 \AA^{-1}) are displayed together to facilitate comparison.



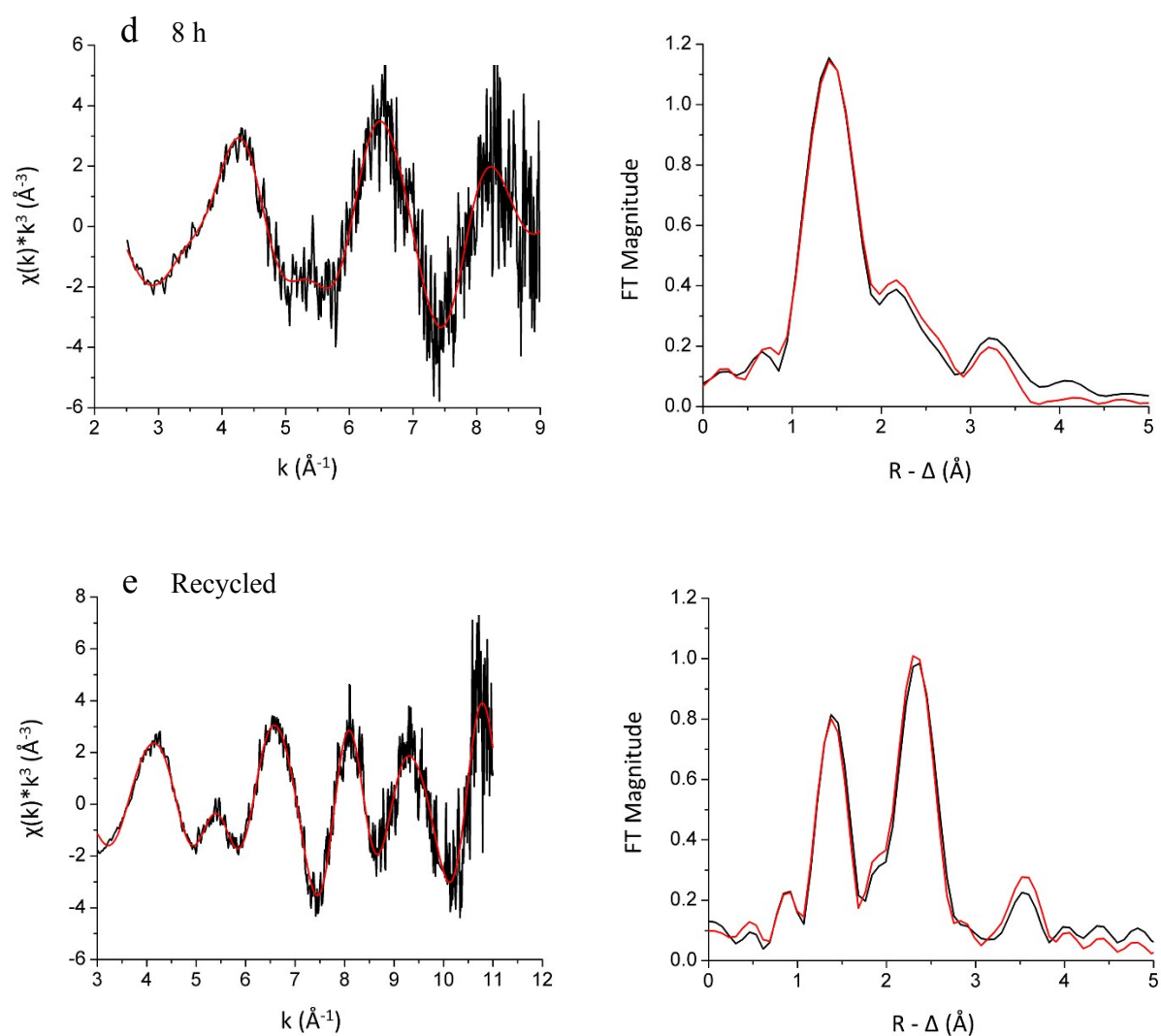
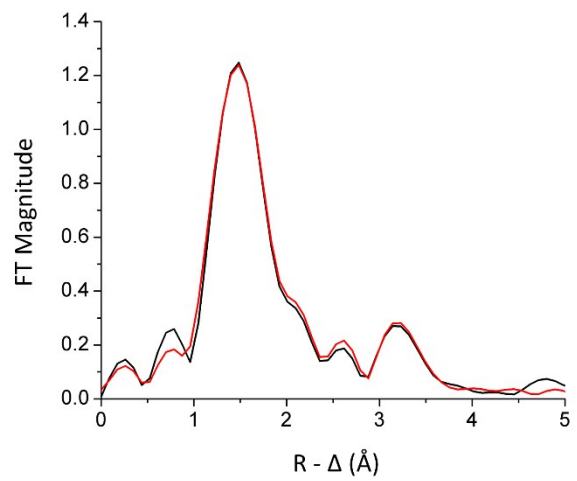
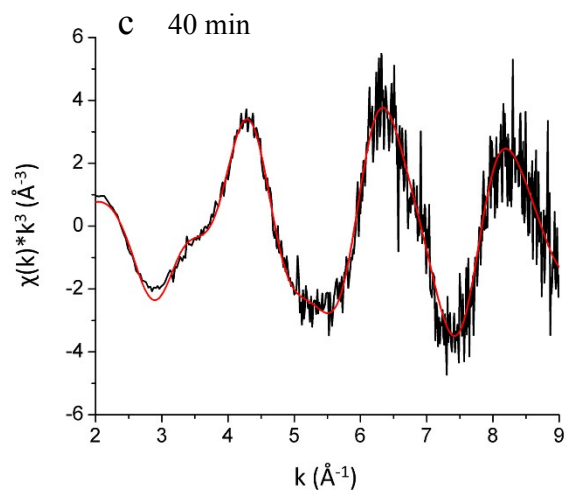
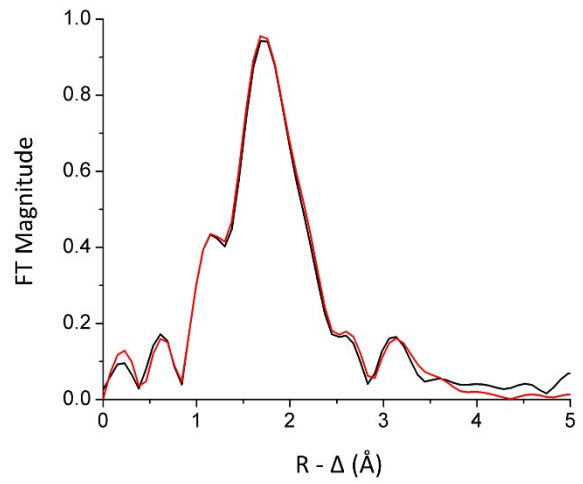
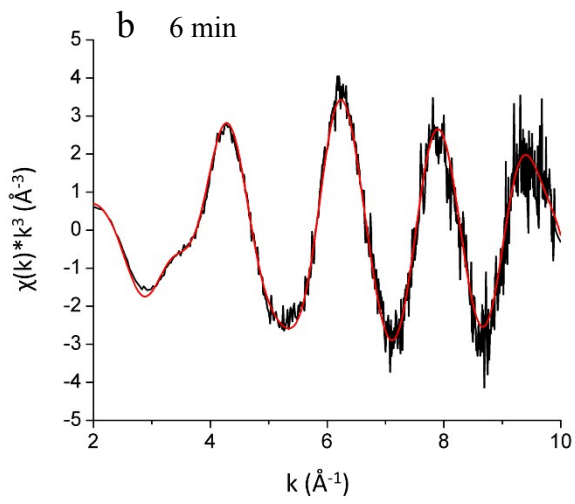


Figure S4. Fit of Pd *K*-edge EXAFS spectra (left) and the Fourier transforms (right) of (a) as-synthesized **1**@rGO, (b) 6 min, (c) 3.5 h, (d) 8 h of the *in situ* measurement and (e) recycled **1**@rGO, black curve – experimental, red curve – model.

a As-synthesized **1**



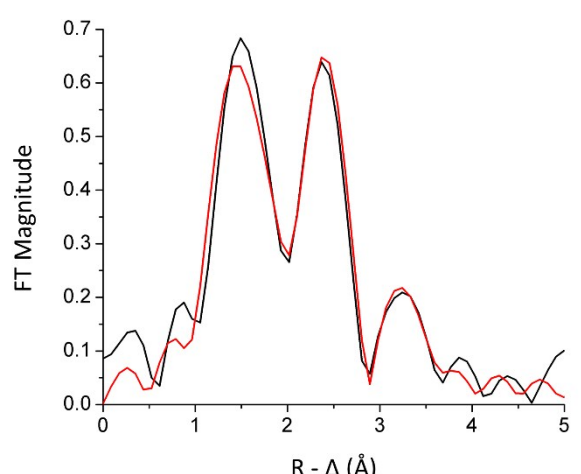
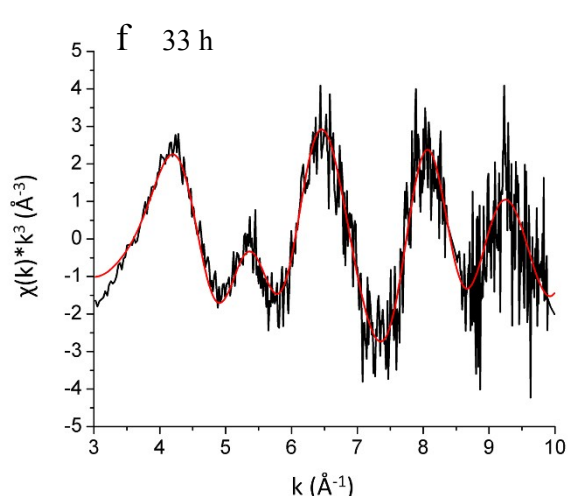
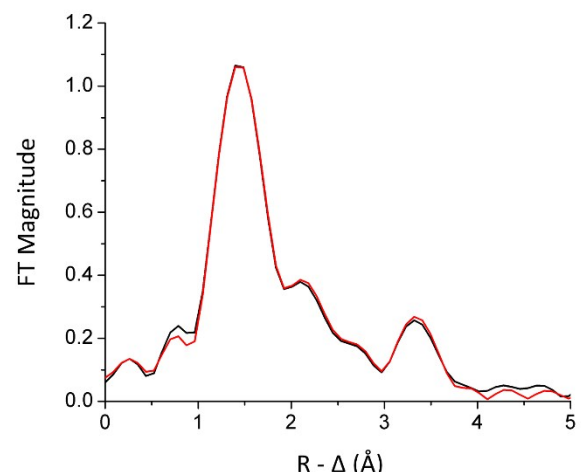
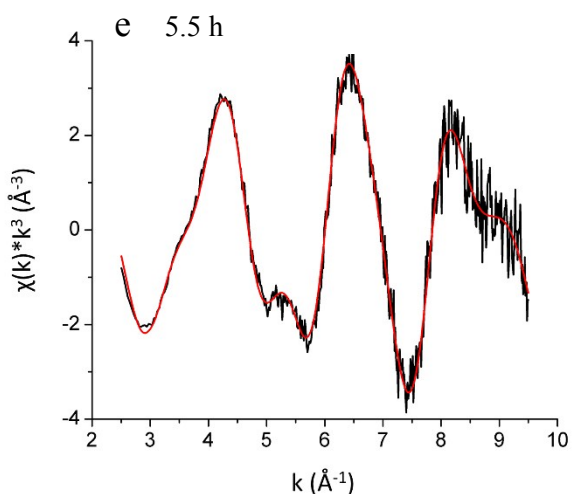
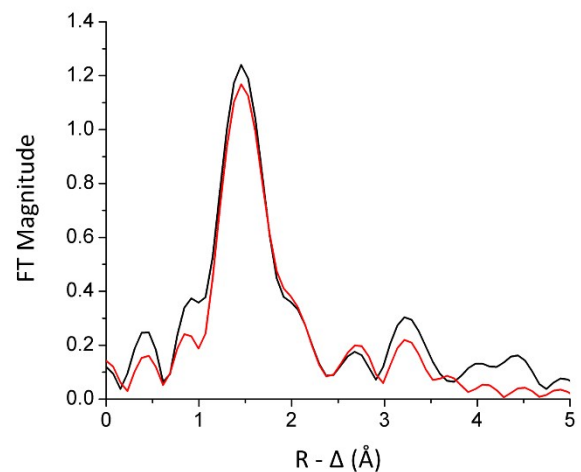
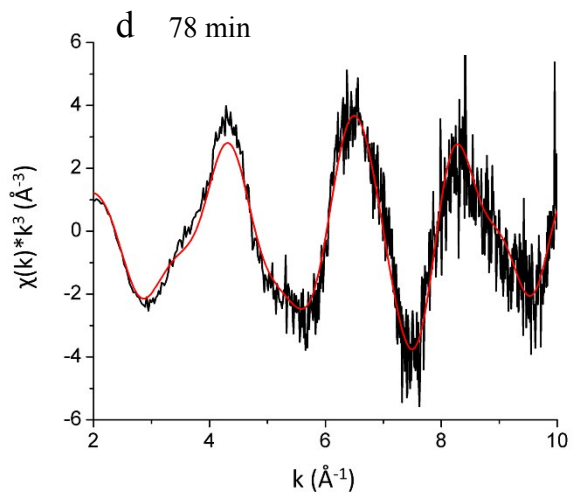


Figure S5. Fit of Pd *K*-edge EXAFS spectra (left) and the Fourier transforms (right) of (a) as-synthesized **1**, (b) 6 min, (c) 40 min, (d) 78 min, (e) 5.5 h and (f) 33 h of the *in situ* measurement, black curve – experimental, red curve – model.

Section S4. Transmission electron microscopy images of recycled **1**@rGO.

Transmission electron microscopy (TEM) data was collected using a JEM-3000F microscope, equipped with a field-emission gun, and operated at 300 kV. High resolution TEM (HRTEM) images were recorded to determine possible crystallinity of the sample, and scanning TEM (STEM) imaging were used to show atomic number contrast as well as to record elemental mapping. X-ray energy dispersive spectroscopy (EDS, Oxford Instruments) was used for elemental mapping recording elemental maps as well as qualitative analysis. The sample was dispersed in ethanol and a TEM-sample grid (made of Cu and covered with a lacy carbon film) was dipped into the dispersion (to retrieve the sample).

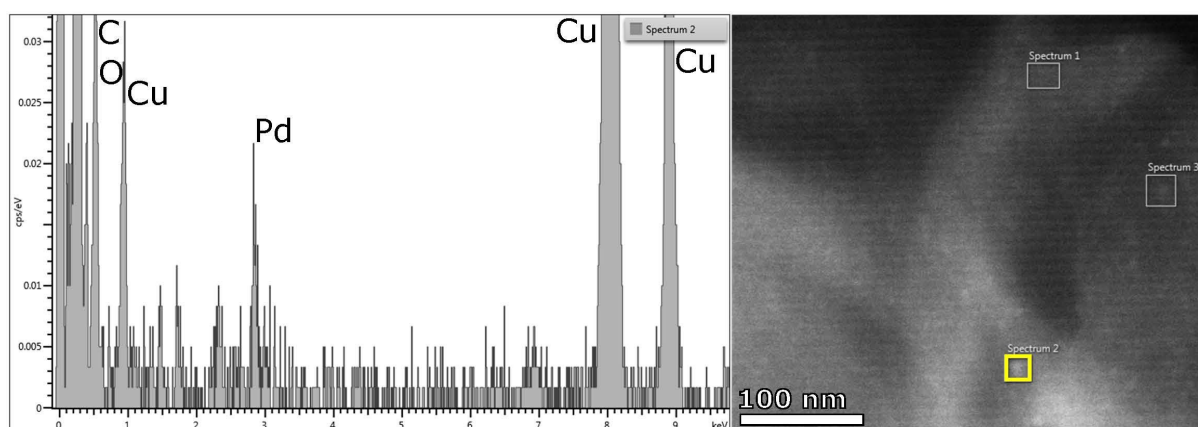


Figure S6. EDS spectrum and STEM image showing a typical area of acquisition on the rGO. The signal is low due to the very thin sample but the Pd-signal is clearly distinguishable. The analysis shows the presence of Pd, well dispersed over the whole sample of the rGO.

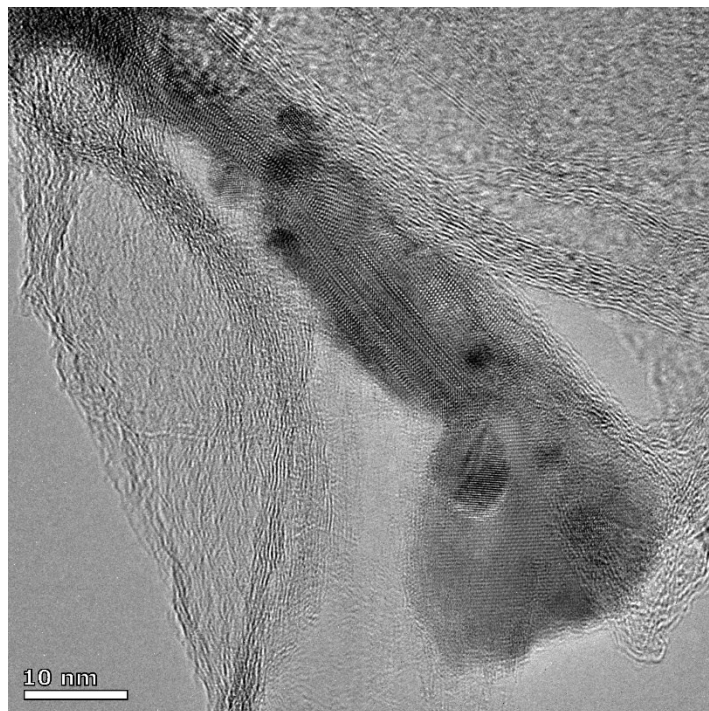


Figure S7. A HRTEM image of a rod-like particle found together with the rGO. The rGO is seen in the left part of the image as transparent sheets with curled-up edges. The rod-like particle is crystalline with some crystalline nanoparticles covering its surface. More particles of the same kind are found throughout the sample, and they are always covered by the smaller nanoparticles, which are up to 10 nanometers in diameter.

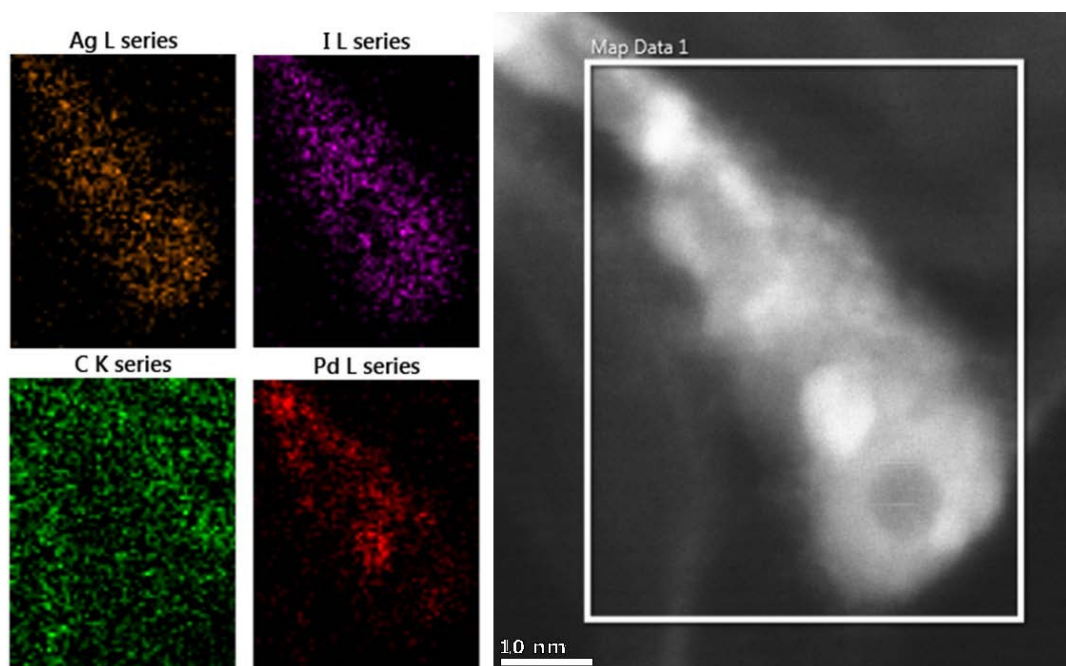


Figure S8. Elemental maps recorded by EDS of the particle imaged in figure S8. The STEM-image to the right is formed using the high-angle annular dark-field (HAADF) detector in which the denser particles appear with more intensity compared to the thin rGO in the background. The elemental maps for elements Ag, I, C and Pd respectively are formed using the TruMap-routine in Oxford Instrument's Aztec software (which eliminates the overlap of peaks for Ag and Pd). The results suggest that the rod-like object consists of Ag and I, and the particles on its surfaces are Pd.

Note: The source of Ag might be from the AgCl as a contaminant during the synthesis of **1**, and the use of $\text{PhI}(\text{OAc})_2$ may give rise to AgI which is highly insoluble and could be concentrated in some parts of the catalyst.

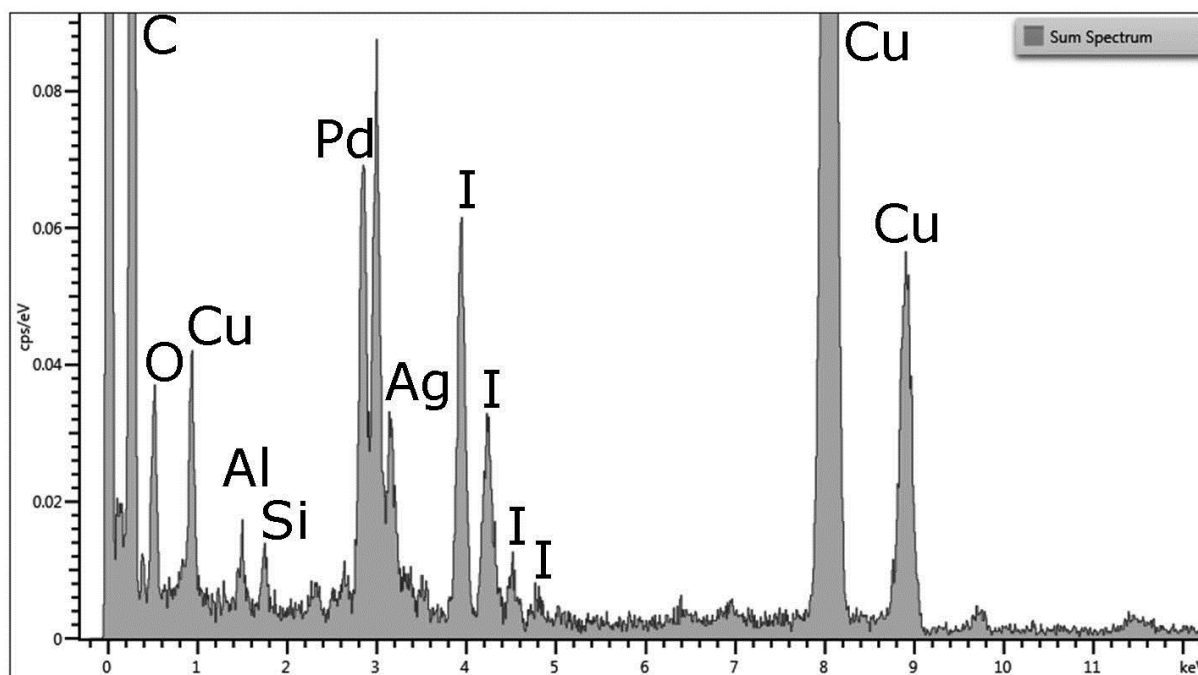


Figure S9. The full EDS-spectrum for the area analyzed in figure S9. The Cu-peaks are associated with the sample grid. Si and Al signals are both low and not spatially associated with any part of the mapped area which leads to the conclusion that they are not part of the object. The L-peaks of Pd and Ag overlaps but both elements are confirmed. This is most easily seen at the peak at ~ 3 keV (consisting of both Pd-L β 1 and Ag-L α) being higher than the peak at ~ 2.8 keV (Pd-L α), which would not be the case of pure Pd. This means there must be some Ag present.

References

- (1) A. Thompson, D. Atwood, E. Gullikson, M. Howells, K.-J. Kim, J. Kirz, J. Kortright, I. Lindau, Y. Liu, P. Pianatta, A. Robinson, J. Scofield, J. Underwood, G. Williams and H. Winick, *X-ray Data Booklet*, LBNL/PUB-490 Rev. 3, Lawrence Berkeley National Laboratory, Berkeley, California 94720, 2009.
- (2) N. Heidenreich, U. Rütt, M. Köppen, A. K. Inge, S. Beier, A.- C. Dippel, R. Suren and N. Stock, *Rev. Sci. Instrum.*, 2017, **88**, 104102.
- (3) G. N. George, I. J. Pickering, EXAFSPAK – A Suite of Computer Programs for Analysis of X-ray Absorption Spectra, SSRL, Stanford, CA. 1993.
- (4) S. I. Zabinsky, J. J. Rehr, A. Ankudinov, R. C. Albers, M. J. Eller, *Phys. Rev. B* 1995, **52**, 2995–3009.
- (5) M. H. Majeed, P. Shayesteh, A. R. Persson, L. R. Wallenberg, J. Schnadt and O. F. Wendt, *Eur. J. Inorg. Chem.*, 2018, 4742–4746.